



## Measurement of transient atomic displacements in thin films with picosecond and femtometer resolution

M. Kozina, T. Hu, J. S. Wittenberg, E. Szilagyi, M. Trigo, T. A. Miller, C. Uher, A. Damodaran, L. Martin, A. Mehta, J. Corbett, J. Safranek, D. A. Reis, and A. M. Lindenberg

Citation: *Structural Dynamics* **1**, 034301 (2014); doi: 10.1063/1.4875347

View online: <http://dx.doi.org/10.1063/1.4875347>

View Table of Contents: <http://scitation.aip.org/content/aca/journal/sdy/1/3?ver=pdfcov>

Published by the American Crystallographic Association, Inc.

---

### Articles you may be interested in

[Phase transition studies in bismuth ferrite thin films synthesized via spray pyrolysis technique](#)

AIP Conf. Proc. **1536**, 1061 (2013); 10.1063/1.4810600

[Atomic vapor deposition of bismuth titanate thin films](#)

J. Appl. Phys. **113**, 187207 (2013); 10.1063/1.4801985

[Composition measurement of the Ni-silicide transient phase by atom probe tomography](#)

Appl. Phys. Lett. **96**, 261904 (2010); 10.1063/1.3457995

[A microprobe technique for simultaneously measuring thermal conductivity and Seebeck coefficient of thin films](#)

Appl. Phys. Lett. **96**, 062107 (2010); 10.1063/1.3300826

[Reliable thin film encapsulation for organic light emitting diodes grown by low-temperature atomic layer deposition](#)

Appl. Phys. Lett. **94**, 233305 (2009); 10.1063/1.3153123

---

## Measurement of transient atomic displacements in thin films with picosecond and femtometer resolution

M. Kozina,<sup>1,2</sup> T. Hu,<sup>3,4</sup> J. S. Wittenberg,<sup>4</sup> E. Szilagyi,<sup>4,5</sup> M. Trigo,<sup>1,4</sup>  
T. A. Miller,<sup>3,4</sup> C. Uher,<sup>6</sup> A. Damodaran,<sup>7</sup> L. Martin,<sup>7</sup> A. Mehta,<sup>8</sup> J. Corbett,<sup>8</sup>  
J. Safranek,<sup>8</sup> D. A. Reis,<sup>1,2,4</sup> and A. M. Lindenberg<sup>1,3,4</sup>

<sup>1</sup>Stanford PULSE Institute, SLAC National Accelerator Laboratory, Menlo Park, California 94025, USA

<sup>2</sup>Department of Applied Physics, Stanford University, Stanford, California 94305, USA

<sup>3</sup>Department of Materials Science and Engineering, Stanford University, Stanford, California 94305, USA

<sup>4</sup>Stanford Institute for Materials and Energy Sciences, SLAC National Accelerator Laboratory, Menlo Park, California 94025, USA

<sup>5</sup>Department of Chemistry, Stanford University, Stanford, California 94305, USA

<sup>6</sup>Department of Physics, University of Michigan, Ann Arbor, Michigan 48109, USA

<sup>7</sup>Department of Materials Science and Engineering, University of Illinois Urbana Champaign, Urbana, Illinois 61801, USA

<sup>8</sup>Stanford Synchrotron Radiation Lightsource, SLAC National Accelerator Laboratory, Menlo Park, California 94025, USA

(Received 15 March 2014; accepted 25 April 2014; published online 6 May 2014)

We report measurements of the transient structural response of weakly photo-excited thin films of BiFeO<sub>3</sub>, Pb(Zr,Ti)O<sub>3</sub>, and Bi and time-scales for interfacial thermal transport. Utilizing picosecond x-ray diffraction at a 1.28 MHz repetition rate with time resolution extending down to 15 ps, transient changes in the diffraction angle are recorded. These changes are associated with photo-induced lattice strains within nanolayer thin films, resolved at the part-per-million level, corresponding to a shift in the scattering angle three orders of magnitude smaller than the rocking curve width and changes in the interlayer lattice spacing of fractions of a femtometer. The combination of high brightness, repetition rate, and stability of the synchrotron, in conjunction with high time resolution, represents a novel means to probe atomic-scale, near-equilibrium dynamics. © 2014 Author(s). All article content, except where otherwise noted, is licensed under a Creative Commons Attribution 3.0 Unported License. [<http://dx.doi.org/10.1063/1.4875347>]

For over a decade, femtosecond to picosecond atomic-scale dynamical processes in matter have been probed using pulsed x rays from sources ranging from laboratory-scale to synchrotrons to free electron lasers.<sup>1–5</sup> However, these experiments have been constrained in most cases by low repetition rates, insufficient brightness, long pulse durations, and/or large pulse-to-pulse fluctuations, necessitating the examination of systems driven far from equilibrium in order to generate a measurable signal. Recent efforts at synchrotrons have begun to develop capabilities for high repetition rate dynamical studies, but have largely been constrained to 100 ps time resolution and/or large excitation fluences.<sup>6–14</sup> The development of techniques that enable atomic-scale resolution, real-time probes of materials and devices in a regime relevant to the phase space occupied by materials near equilibrium is therefore an important research direction. For example, phonon transport across interfaces in thin films or heterostructures intrinsically involves picosecond transport processes and resultant part-per-million strains.<sup>5,10,15,16</sup> Here, we show that by utilizing the high brightness, repetition rate, and stability of a synchrotron, one may use x-ray scattering techniques to probe the atomic-scale dynamics and phonon conduction processes within systems close to equilibrium with 15 ps time resolution, corresponding to photo-induced lattice changes at the 10<sup>–6</sup> level, applicable to broad diffraction peaks associated with nanoscale systems.

We present measurements probing transient photo-induced strain as encoded in shifts of diffraction peaks in several thin film materials. Three specific samples were examined: c-axis

bismuth (130 nm) on sapphire, monodomain BiFeO<sub>3</sub> (60 nm, [110] orientation) on SrTiO<sub>3</sub> (BFO/STO), and Pb(Zr,Ti)O<sub>3</sub> (100 nm, [001]) on SrRuO<sub>3</sub>:SrTiO<sub>3</sub>:Si (PZT/SRO/STO/Si). Bismuth has primarily been studied via time-resolved x-ray diffraction in the strongly pumped regime at sub-10 kHz repetition rates.<sup>1,3,6,17–19</sup> BFO and PZT are multiferroic and ferroelectric materials, respectively, and exhibit novel photoferroelectric responses<sup>20–27</sup> associated with coupling between currents, electric fields, and strain with the fundamental time-scales for these processes not well understood. The PZT sample additionally served as a lower bound for the time resolution of the experiment.

Measurements were conducted in a standard pump-probe x-ray scattering geometry at the Stanford Synchrotron Radiation Lightsource at beamline 10-2 using monochromatized 10 and 12 keV (with approximately 5 eV bandwidth) x rays with  $\sim 200 \mu\text{Rad}$  divergence as a probe, and a femtosecond optical laser synchronized to the electron bunches in the ring as a pump. Experiments were performed in two distinct modes of operation with different temporal characteristics: 1. standard operation mode, with x-ray pulses of 60 ps full-width half maximum (FWHM) in duration; 2. low- $\alpha$  mode, with 15 ps FWHM pulses. In the low- $\alpha$  mode, the trajectory of the electron bunches in the ring is altered to yield shorter duration x-ray pulses at reduced bunch currents.<sup>28,29</sup> In both operating modes, the fill pattern of the synchrotron consisted of four pulse trains, roughly 20 ns apart, with individual pulses in each train separated by 2.1 ns, accompanied by a single timing pulse separated from any other pulse by 60 ns on either side at 1.28 MHz repetition rate (the inverse round trip time of the storage ring); see Fig. 1. A Pilatus 100 K area detector<sup>30</sup> was used to collect the scattered x rays from the timing pulse enabling pump-probe measurements limited by the duration of the x-ray pulse. The flux from the timing pulse was  $2.6 \times 10^9/\text{s}$  in regular operations and reduced by roughly a factor of 15 in low- $\alpha$  mode. X rays with a spot size of  $150 \times 240 \mu\text{m}^2$  were incident on the sample at approximately the Bragg condition and only symmetric thin film reflections were probed.

A 1.28 MHz, 500 fs FWHM,  $2 \mu\text{J}$  per pulse Er-doped fiber laser with fundamental wavelength 1030 nm was used as the optical pump source, phase locked to the 476 MHz electron bunch RF signal. Time scans were carried out by delaying the 476 MHz RF signal using a variable length RF transmission line. Both the fundamental wavelength of the laser (1030 nm) and the second harmonic (515 nm) were used to pump the semimetallic Bi film sample, whereas the laser was frequency tripled to 343 nm to excite above bandgap for BFO and PZT.<sup>31,32</sup> The typical absorbed fluence for the Bi sample was  $210 \mu\text{J}/\text{cm}^2$  (1030 nm) and  $75 \mu\text{J}/\text{cm}^2$  (515 nm) while for the BFO and PZT it was  $\sim 25 \mu\text{J}/\text{cm}^2$ , with the harmonics filtered appropriately via dielectric mirrors. The ratio of x-ray probe to laser pump spot area was roughly 1:3, 1:2, and 1:1 for the 1030 nm, 515 nm, and 343 nm light, respectively.

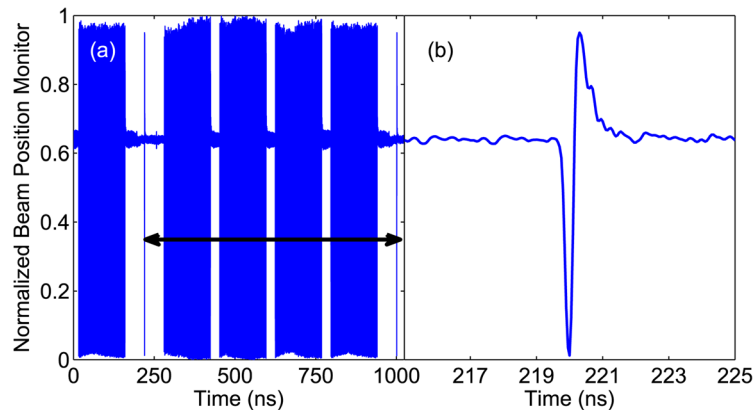


FIG. 1. (a) Beam position monitor illustrating time structure of x-ray bunches. There are four pulse trains per synchrotron period (781 ns) consisting of pulses 2.1 ns apart along with one lone bunch separated by a  $\sim 60$  ns gap on either side. This bunch alone is used for timing. The black arrow shows one round trip of the synchrotron. (b) Zoomed-in portion of (a) centered around the timing pulse; fine time structure is an artifact of the detection mechanism.

In the standard operating mode, the Bi film was excited at 1030 nm recording the symmetric 222 reflection (rhombohedral cell) via diffraction in a Bragg geometry with scattering in the vertical plane. Note the Bi sample was also pumped with 515 nm light but was probed in the short-pulse, low- $\alpha$  mode; see below for more discussion. The diffracted x-ray spot was recorded on the area detector such that measurements of photo-induced changes in the angular position of the center of mass<sup>33</sup>  $\Theta_{com}$  and higher order moments were extracted as a function of time-delay between pump and probe. From a change in  $\Theta_{com}$  changes in the lattice parameter can be extracted. This change has subtle dependence on both the crystal acceptance and beam divergence, as well as a small dependence on deviation from the symmetric scattering geometry.<sup>34</sup> Specifically for a symmetric geometry

$$\frac{\Delta d}{d} = -\Delta\Theta_{com} \left\{ \frac{1}{[1 - f(\nu)]\tan\theta_b + f(\nu)\sin 2\theta_b} \right\}, \quad (1)$$

where  $\theta_b$  is the nominal Bragg angle,  $\nu$  is the ratio of the rocking curve width to the incoming beam divergence, and  $f(\nu)$  is given by

$$f(\nu) = \frac{\nu^2}{\nu^2 + \sin^2\theta_b}. \quad (2)$$

Note  $f(\nu)$  is a monotonic function that goes to 0 when the beam divergence is much larger than the rocking curve width and goes to 1 in the plane wave limit. When the rocking curve width is much larger than the incident beam angular divergence ( $\nu \gg 1$ ) as is realized by our experimental parameters ( $\nu = 50$ , rocking curve width  $0.5^\circ$ ), there is a direct mapping between the shift in angular center of mass of the x-ray diffraction pattern and the change in lattice spacing. We predict this mapping to be weakly sensitive to small deviations in the incident x-ray direction from the Bragg angle. See the supplementary material for more details concerning geometries slightly off the symmetric condition (Ref. 34). Moreover, in this limit, the effects of the finite energy spread in the beam are also negligible. For the Bi film, a clear deflection of the x-ray beam is observed within the scattering plane, corresponding to smaller scattering angles, from which changes in the lattice parameter are directly extracted.

In Fig. 2(a) we show a 1D lineout of the area detector as a function of time delay with the average x-ray early (i.e., optical pump arriving after x-ray probe) trace subtracted to highlight differences. Note the clear shift in peak center when the x rays come just after the laser. Fig. 2(b) shows the time-dependent fractional change in the Bi lattice parameter as determined from  $\Delta\Theta_{com}$  and Eq. (1). The noise level corresponds to strains less than  $10^{-6}$ . We observe an initial increase in the lattice parameter followed by a partial recovery and damped oscillations. A fit to an error function for the rise time yields  $65 \pm 15$  ps (FWHM), consistent with the time resolution of the x-ray pulses and therefore indicative of lattice changes in the Bi occurring at a rate much faster than the x rays. This time-scale is comparable to acoustic propagation time through the film (using  $c_l = 1.9$  nm/ps (Ref. 35)). Motivated by Refs. 18 and 35, we fit the long-time recovery to a decaying exponential yielding a time-constant of  $4.8 \pm 0.3$  ns. Assuming a 1D diffusion model with a thermal boundary (Kapitza) conductance between the Bi film and sapphire substrate (similar to Ref. 18), we extract from this time constant a Kapitza conductance  $\sigma_k = 3.2 \pm 0.2$  kW/cm<sup>2</sup>K for the Bi/Sapphire interface roughly consistent with the value of 1.95 kW/cm<sup>2</sup>K extracted in Ref. 18. There is additionally an observed change in the square root of the variance of the x-ray intensity distribution (defined as  $\sqrt{\langle x^2 \rangle - \langle x \rangle^2}$ , where  $x$  is the angular coordinate on the detector) corresponding to a time-dependent broadening followed by a slower nanosecond recovery as shown in the inset to Fig. 2(b). This is consistent with increased mosaicity or inhomogeneous strain induced by the laser.<sup>26</sup>

Further measurements were carried out probing photo-induced strain dynamics in BFO thin films at excitation fluences of  $\sim 25$   $\mu$ J/cm<sup>2</sup>. Fig. 3 shows time-resolved changes observed in both the BFO thin film (a,c) and the STO substrate (b,c). Figs. 3(a) and 3(b) show a 2D plot of

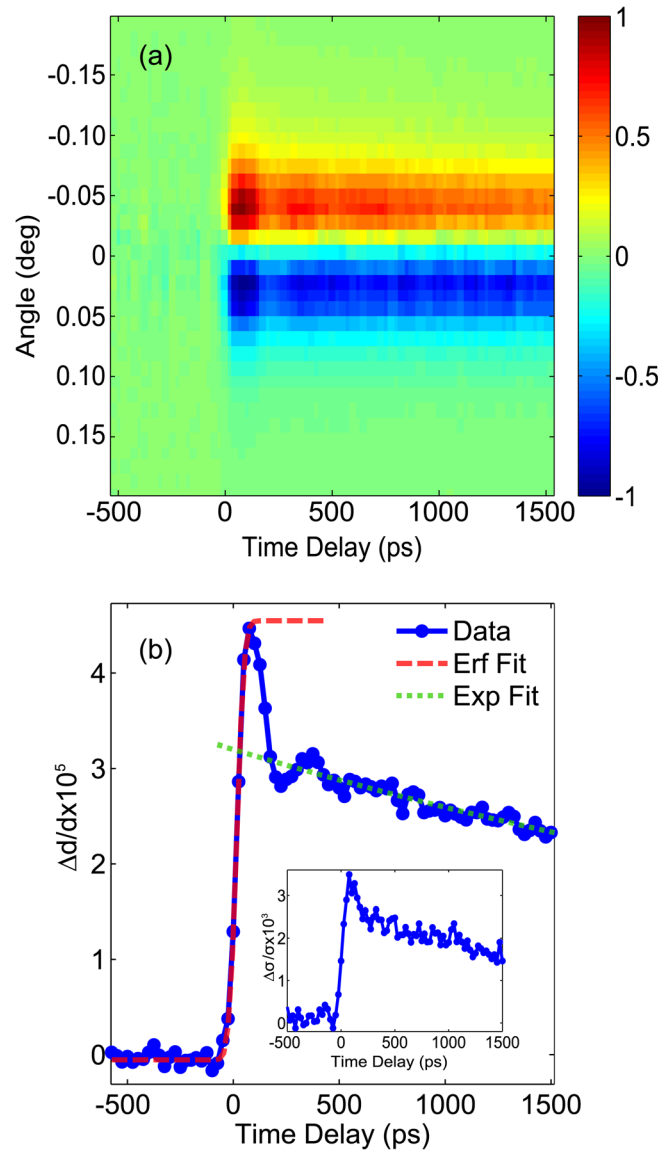


FIG. 2. (a) 2D plot of the Bi 222 diffraction peak shift induced by  $210 \mu\text{J}/\text{cm}^2$  of 1030 nm laser light. The vertical axis is a summation across the area detector mapping the 2D detector to an angular lineout. The horizontal axis is the time delay between laser and x-ray pulses (negative time means x rays arrive first). The intensity axis is the difference (normalized to  $\pm 1$ ) between the averaged lineout with x rays very early (before any excitation, i.e., negative time) and the lineout at each particular time point. (b) Fractional change in Bi lattice spacing  $\Delta d/d$  extracted from data in (a). The dashed red line is an error function (“Erf”) fit for the initial change. The dotted green line is an exponential (“Exp”) decay fit on long time-scales. The inset shows the fractional change in the square root of the variance of the x-ray distribution on the detector along the scattering plane direction.

change in angular position of the peak vs time in the same form as Fig. 2(a), while Fig. 3(c) shows the fractional change in lattice spacing for both the BFO and STO. In the BFO, we see a shift in the position of the diffracted 220 BFO reflection, associated with an expansion of the thin film, as has been observed before at 20 times higher fluences.<sup>24,27</sup> An error function fit yields a rise time of  $75 \pm 15$  ps. By additionally recording changes in the STO 220 substrate reflection we resolve the time-scale for energy transfer across the BFO-STO interface manifested as a  $920 \pm 140$  ps delay between the BFO response and the STO response. Consistent with our Bi/sapphire data above as well as with Refs. 18 and 35, the delayed onset of a change in the STO peak is indicative that there is a non-negligible thermal boundary resistance at the

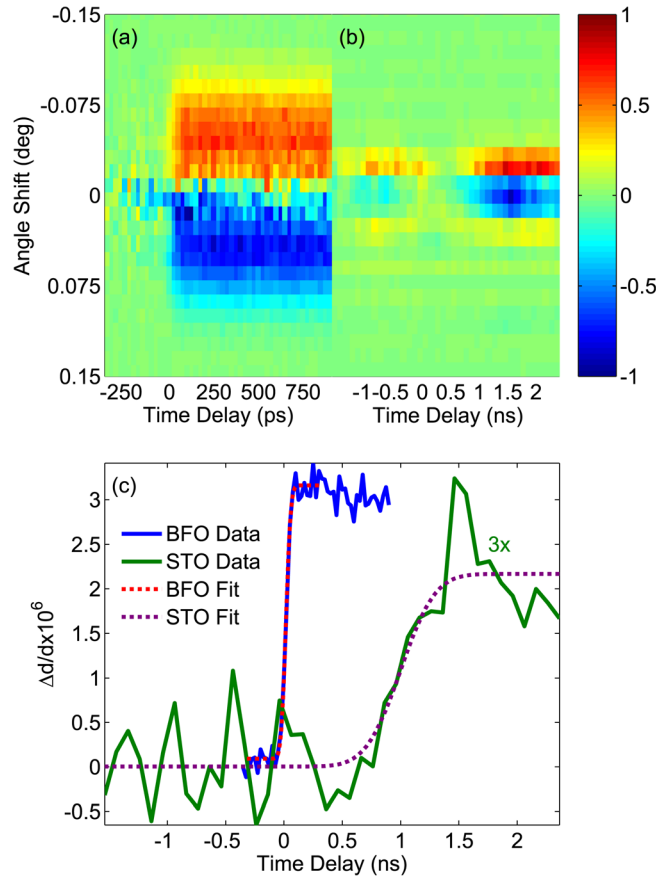


FIG. 3. (a) 2D plot of the BFO film 220 diffraction peak shift upon excitation by 343 nm optical pulse ( $25 \mu\text{J}/\text{cm}^2$  absorbed). The vertical axis is a summation across the area detector mapping the 2D detector to an angular lineout. The horizontal axis is time delay between laser and x rays. The intensity axis is the difference (normalized to  $\pm 1$ ) between the average lineout with x rays very early (before any excitation) and the lineout at each particular time point. (b) 2D plot similar to (a) for the STO substrate. (c) Fractional change in BFO film (blue) and STO substrate (red) lattice spacings. Red (purple) dashed line is error function fit to the BFO (STO) rise time. There is a clear delay between the temporal overlap of the x-ray and laser pulses ( $\sim t=0$ ) and the actual onset of a change in the STO, while the change in the BFO happens immediately. Note the STO data are scaled by a factor of 3 for ease of comparison with the BFO data and are averaged over several neighboring times for smoothing.

BFO/STO interface. This results in heat transfer from the BFO to the STO occurring on time-scales much longer than for simple acoustic propagation. In contrast to the work in Refs. 18 and 35, though, we resolve here the structural changes in the substrate itself. The magnitude of the observed strain in the STO film is approximately  $10^{-6}$  averaged over the x-ray extinction depth of the material, a factor of three weaker than for BFO.

In the low- $\alpha$  mode, the momentum compaction factor  $\alpha$ , a measure of the relative change in electron orbit length for fractional changes in electron momentum,<sup>28</sup> is reduced such that the overall electron bunch duration, which scales as approximately  $\sqrt{\alpha}$ , decreases. This is done at the expense of some loss in bunch current in order to mitigate increased impedance associated with the vacuum chamber and coherent synchrotron radiation. For these experiments, we ran in an  $\alpha/18$  mode associated with a factor of 4 reduction in the normal synchrotron pulse duration. Streak camera measurements confirmed  $\sim 15$  ps FWHM x-ray pulses (Fig. 4(a) inset). Fig. 4 shows the induced fractional lattice change for the PZT, Bi, and BFO samples (excited with 343 nm, 515 nm, and 343 nm light, respectively) measured in this short pulse mode. The respective reflections measured were the 003, 222, and 220 peaks.

The PZT thin film shows a photo-induced expansion along the c-axis (the ferroelectric polarization direction) comparable to measurements for the Bi and BFO samples. The data are

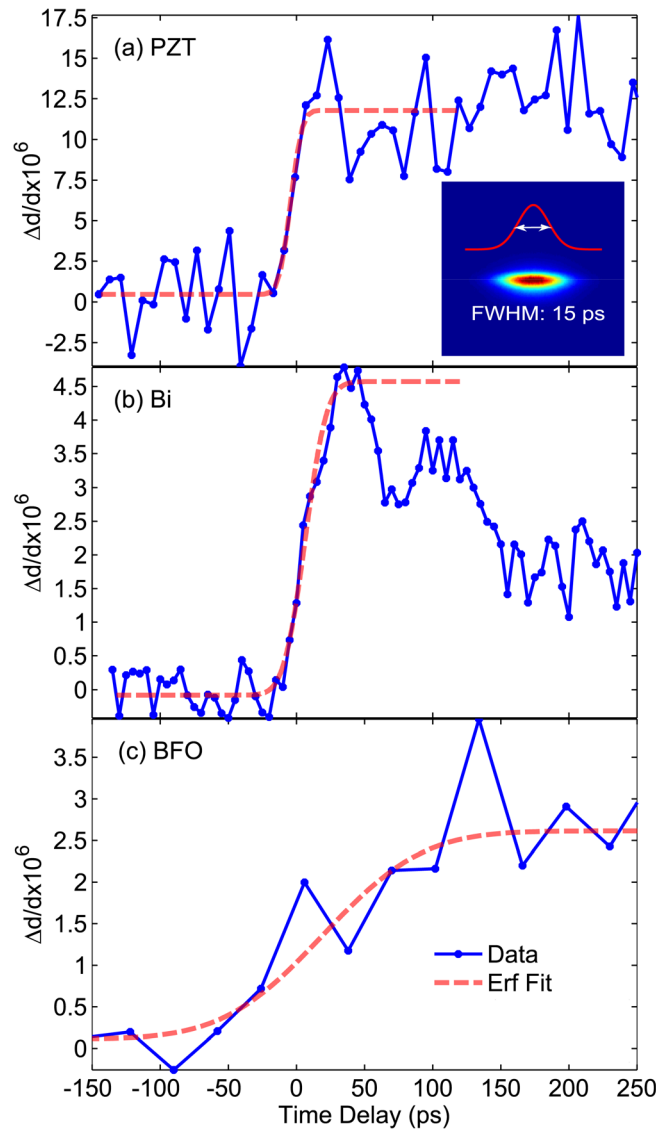


FIG. 4. Fractional changes in (a) PZT, (b) Bi, and (c) BFO lattice spacings  $\Delta d/d$  measured with the 003, 222, and 220 reflections, respectively, collected in the short-pulse, low- $\alpha$  mode. The inset to (a) shows streak camera data measuring the x-ray pulse duration in the low- $\alpha$  mode. The BFO and PZT samples were pumped with an absorbed fluence of  $25 \mu\text{J}/\text{cm}^2$  of 343 nm light and the Bi sample with  $75 \mu\text{J}/\text{cm}^2$  of 515 nm light. The red dashed line is a fit to an error function for all three samples.

displayed on the same time axis to allow visual comparison of rise times. A fit of the PZT expansion to an error function reveals a FWHM rise time of  $\sim 15$  ps, consistent with measurements limited by the x-ray pulse duration. These results are in agreement with previous studies on  $\text{PbTiO}_3$  films that show acoustically limited expansion dynamics using an x-ray free electron laser.<sup>20</sup> Similar to Ref. 20, the observed expansion is opposite to what would be expected based on thermal heating, in which the c-axis tetragonality is reduced as the temperature is increased closer to the Curie temperature. The 515-nm-pumped Bi sample also shows a rapid rise time, with a fit yielding  $\sim 29$  ps, indicating a similarly fast response, with well-defined acoustic oscillations following time zero.<sup>6</sup>

In contrast, the dynamical response of BFO measured in the low- $\alpha$  mode shows expansion dynamics occurring on a much slower time-scale (Fig. 4(c)), consistent with the normal operations data. These time-scales are significantly slower than previous measurements taken at

much higher fluences ( $\sim 1$  order of magnitude) indicative of two different excitation regimes. At low fluences, the observed response is slower even than the acoustic propagation time across the film ( $\sim 20$  ps) suggesting that the photo-induced response is not purely driven by simple thermally driven longitudinal expansion and likely involves coupling to in-plane strains which will necessarily evolve on slower time-scales.<sup>24,26,27</sup>

In conclusion, methods for performing time-resolved x-ray diffraction experiments at a high repetition rate ( $>1$  MHz) have been established in a weakly perturbative regime utilizing the high brightness of a synchrotron source with time resolution down to 15 ps and with strain sensitivity at the  $10^{-6}$  level, corresponding to changes in the interlayer lattice spacing of fractions of a femtometer, and applicable to weakly scattering, nanolayer thin films. In particular, strains of this magnitude correspond to net displacements at the 100 fm level for a 100 nm thin film. These measurements reveal the first steps in interfacial thermal transport and allow for extraction of associated interfacial Kapitza conductances in complex heterostructures in the near-equilibrium limit. In ferroelectric nanolayers, these measurements reveal photoferroelectric effects associated with photo-induced, acoustically driven lattice strains in PZT in comparison with a slower dynamical response in BFO.

The authors wish to thank Valery Borzenets for help with the experimental setup, as well as the LCLS Laser Science and Technology Division for expertise and equipment. This work was supported by the U.S. Department of Energy, Office of Science, Basic Energy Sciences, Materials Sciences and Engineering Division. Portions of this research were carried out at the Stanford Synchrotron Radiation Lightsource, a Directorate of SLAC National Accelerator Laboratory and an Office of Science User Facility operated for the U.S. Department of Energy Office of Science by Stanford University. M.K. was supported in part by an award from the Department of Energy (DOE) Office of Science Graduate Fellowship Program (DOE SCGF). D.A.R. was supported in part by the Air Force Office of Scientific Research under Contract No. FA9550-08-1-0340 through the Multidisciplinary University Research Initiative Program. The growth of Bi films at UM was supported by the Center for Solar and Thermal Energy Conversion, an Energy Frontier Research Center funded by the U.S. Department of Energy, Office of Basic Energy Sciences under Award No. DE-SC0000957. The growth of BFO films at UIUC was supported by the Army Research Office under Grant No. W911NF-10-1-0482. Early stages of this work were supported by the Department of Energy, Laboratory Directed Research and Development funding, under Contract No. DE-AC02-76SF00515.

<sup>1</sup>K. Sokolowski-Tinten, C. Blome, C. Dietrich, A. Tarasevitch, M. H. von Hoegen, D. von der Linde, A. Cavalleri, J. Squier, and M. Kammler, "Femtosecond x-ray measurement of ultrafast melting and large acoustic transients," *Phys. Rev. Lett.* **87**, 225701 (2001).

<sup>2</sup>A. M. Lindenberg, I. Kang, S. L. Johnson, T. Missalla, P. A. Heimann, Z. Chang, J. Larsson, P. H. Bucksbaum, H. C. Kapteyn, H. A. Padmore, R. W. Lee, J. S. Wark, and R. W. Falcone, "Time-resolved x-ray diffraction from coherent phonons during a laser-induced phase transition," *Phys. Rev. Lett.* **84**, 111–114 (2000).

<sup>3</sup>D. M. Fritz, D. A. Reis, B. Adams, R. A. Akre, J. Arthur, C. Blome, P. H. Bucksbaum, A. L. Cavalieri, S. Engemann, S. Fahy, R. W. Falcone, P. H. Fuoss, K. J. Gaffney, M. J. George, J. Hajdu, M. P. Hertlein, P. B. Hillyard, M. H. von Hoegen, M. Kammler, J. Kaspar, R. Kienberger, P. Krejciak, S. H. Lee, A. M. Lindenberg, B. McFarland, D. Meyer, T. Montagne, E. D. Murray, A. Nelson, M. Nicoul, R. Pahl, J. Rudati, H. Schlarb, D. P. Siddons, K. Sokolowski-Tinten, T. Tschentscher, D. von der Linde, and J. B. Hastings, "Ultrafast bond softening in bismuth: Mapping a solid's interatomic potential with x-rays," *Science* **315**, 633–636 (2007).

<sup>4</sup>M. Trigo, M. Fuchs, J. Chen, M. P. Jiang, M. Cammarata, S. Fahy, D. M. Fritz, K. Gaffney, S. Ghimire, A. Higginbotham, S. L. Johnson, M. E. Kozina, J. Larsson, H. Lemke, A. M. Lindenberg, G. Ndabashimiye, F. Quirin, K. Sokolowski-Tinten, C. Uher, G. Wang, J. S. Wark, D. Zhu, and D. A. Reis, "Fourier-transform inelastic x-ray scattering from time- and momentum-dependent phonon-phonon correlations," *Nat. Phys.* **9**, 790–794 (2013).

<sup>5</sup>M. Highland, B. C. Grundrum, Y. K. Koh, R. S. Averback, D. G. Cahill, V. C. Elarde, J. J. Coleman, D. A. Walko, and E. C. Landahl, "Ballistic-phonon heat conduction at the nanoscale as revealed by time-resolved x-ray diffraction and time-domain thermoreflectance," *Phys. Rev. B* **76**, 075337 (2007).

<sup>6</sup>C. Laulhé, M. Cammarata, M. Servol, R. J. D. Miller, M. Hada, and S. Ravy, "Impact of laser on bismuth thin-films," *Eur. Phys. J.: Spec. Top.* **222**, 1277–1285 (2013).

<sup>7</sup>H. A. Navirian, M. Herzog, J. Goldshteyn, W. Leitenberger, I. Vrejoiu, D. Khakhulin, M. Wulff, R. Shayduk, P. Gaal, and M. Bargheer, "Shortening x-ray pulses for pump-probe experiments at synchrotrons," *J. Appl. Phys.* **109**, 126104 (2011).

<sup>8</sup>F. A. Lima, C. J. Milne, D. C. V. Amarasinghe, M. H. Rittmann-Frank, R. M. van der Veen, M. Reinhard, V.-T. Pham, S. Karlsson, S. L. Johnson, D. Grolimund, C. Borca, T. Huthwelker, M. Janousch, F. van Mourik, R. Abela, and M.

- Chergui, "A high-repetition rate scheme for synchrotron-based picosecond laser pump/x-ray probe experiments on chemical and biological systems in solution," *Rev. Sci. Instrum.* **82**, 063111 (2011).
- <sup>9</sup>A. M. March, A. Stickrath, G. Doumy, E. P. Kanter, B. Krässig, S. H. Southworth, K. Attenkofer, C. A. Kurtz, L. X. Chen, and L. Young, "Development of high-repetition-rate laser pump/x-ray probe methodologies for synchrotron facilities," *Rev. Sci. Instrum.* **82**, 073110 (2011).
- <sup>10</sup>R. Shayduk, H. Navirian, W. Leitenberger, J. Goldshteyn, I. Vrejoiu, M. Weinelt, P. Gaal, M. Herzog, C. von Korff Schmising, and M. Bargheer, "Nanoscale heat transport studied by high-resolution time-resolved x-ray diffraction," *New J. Phys.* **13**, 093032 (2011).
- <sup>11</sup>E. M. Dufresne, B. Adams, M. Chollet, R. Harder, Y. Li, H. Wen, S. J. Leake, L. Beitra, X. Huang, and I. K. Robinson, "A technique for high-frequency laser-pump x-ray probe experiments at the aps," *Nucl. Instrum. Methods Phys. Res., Sect. A* **649**, 191–193 (2011).
- <sup>12</sup>H. A. Navirian, R. Shayduk, W. Leitenberger, J. Goldshteyn, P. Gaal, and M. Bargheer, "Synchrotron-based ultrafast x-ray diffraction at high repetition rates," *Rev. Sci. Instrum.* **83**, 063303 (2012).
- <sup>13</sup>H. A. Navirian, D. Schick, P. Gaal, W. Leitenberger, R. Shayduk, and M. Bargheer, "Thermoelastic study of nanolayered structures using time-resolved x-ray diffraction at high repetition rate," *Appl. Phys. Lett.* **104**, 021906 (2014).
- <sup>14</sup>K. Haldrup, G. Vankó, W. Gawelda, A. Galler, G. Doumy, A. M. March, E. P. Kanter, A. Bordage, A. Dohn, T. B. van Driel, K. S. Kjør, H. T. Lemke, S. E. Canton, J. Uhlrig, V. Sundström, L. Young, S. H. Southworth, M. M. Nielsen, and C. Bressler, "Guest-host interactions investigated by time-resolved x-ray spectroscopies and scattering at MHz rates: Solvation dynamics and photoinduced spin transition in aqueous  $\text{Fe}(\text{bipy})_3^{2+}$ ," *J. Phys. Chem. A* **116**, 9878–9887 (2012).
- <sup>15</sup>D. G. Cahill, W. K. Ford, K. E. Goodson, G. D. Mahan, A. Majumdar, H. J. Maris, R. Merlin, and S. R. Phillpot, "Nanoscale thermal transport," *J. Appl. Phys.* **93**, 793–818 (2003).
- <sup>16</sup>M. N. Luckyanova, J. Garg, K. Esfarfani, A. Jandle, M. T. Bulsara, A. J. Schmidt, A. J. Minnich, S. Chen, M. S. Dresselhaus, Z. Ren, E. A. Fitzgerald, and G. Chen, "Coherent phonon heat conduction in superlattices," *Science* **338**, 936–939 (2012).
- <sup>17</sup>D. A. Walko, Y.-M. Sheu, M. Trigo, and D. A. Reis, "Thermal transport in thin films measured by time-resolved, grazing incidence x-ray diffraction," *J. Appl. Phys.* **110**, 102203 (2011).
- <sup>18</sup>Y. M. Sheu, M. Trigo, Y. J. Chien, C. Uher, D. A. Arms, E. R. Peterson, D. A. Walko, E. C. Landahl, J. Chen, S. Ghimire, and D. A. Reis, "Kapitza conductance of bi/sapphire interface studied by depth- and time-resolved x-ray diffraction," *Solid State Commun.* **151**, 826–829 (2011).
- <sup>19</sup>S. L. Johnson, P. Beaud, C. J. Milne, F. S. Krasniqi, E. S. Zilstra, M. E. Garcia, M. Kaiser, D. Grolimund, R. Abela, and G. Ingold, "Nanoscale depth-resolved coherent femtosecond motion in laser-excited bismuth," *Phys. Rev. Lett.* **100**, 155501 (2008).
- <sup>20</sup>D. Daranciang, M. J. Highland, H. Wen, S. M. Young, N. C. Brandt, H. Y. Hwang, M. Vattilana, M. Nicoul, F. Quirin, J. Goodfellow, T. Qi, I. Grinberg, D. M. Fritz, M. Cammarata, D. Zhu, H. T. Lemke, D. A. Walko, E. M. Dufresne, Y. Li, J. Larsson, D. A. Reis, K. Sokolowski-Tinten, K. A. Nelson, A. M. Rappe, P. H. Fuoss, G. B. Stephenson, and A. M. Lindenberg, "Ultrafast photovoltaic response in ferroelectric nanolayers," *Phys. Rev. Lett.* **108**, 087601 (2012).
- <sup>21</sup>S. M. Young, F. Zheng, and A. M. Rappe, "First-principles calculation of the bulk photovoltaic effect in bismuth ferrite," *Phys. Rev. Lett.* **109**, 236601 (2012).
- <sup>22</sup>L. Y. Chen, J. C. Yang, C. W. Luo, C. W. Laing, K. H. Wu, J.-Y. Lin, T. M. Uen, J. Y. Juang, Y. H. Chu, and T. Kobayashi, "Ultrafast photoinduced mechanical strain in epitaxial  $\text{BiFeO}_3$  thin films," *Appl. Phys. Lett.* **101**, 041902 (2012).
- <sup>23</sup>S. Y. Yang, J. Seidel, S. J. Byrnes, P. Shafer, C.-H. Yang, M. D. Rossell, P. Yu, Y.-H. Chu, J. F. Scott, J. W. Ager III, L. W. Martin, and R. Ramesh, "Above-bandgap voltages from ferroelectric photovoltaic devices," *Nat. Nanotechnol.* **5**, 143–147 (2010).
- <sup>24</sup>H. Wen, P. Chen, M. P. Cosgriff, D. A. Walko, J. H. Lee, C. Adamo, R. D. Schaller, J. F. Ihlefeld, E. M. Dufresne, D. G. Schlom, P. G. Evans, J. W. Freeland, and Y. Li, "Electronic origin of ultrafast photoinduced strain in  $\text{BiFeO}_3$ ," *Phys. Rev. Lett.* **110**, 037601 (2013).
- <sup>25</sup>B. Kundys, M. Viret, D. Colson, and D. O. Kundys, "Light-induced size changes in  $\text{BiFeO}_3$  crystals," *Nature Mater.* **9**, 803–805 (2010).
- <sup>26</sup>D. Schick, A. Bojahr, M. Herzog, P. Gaal, I. Vrejoiu, and M. Bargheer, "Following strain-induced mosaicity changes of ferroelectric thin films by ultrafast reciprocal space mapping," *Phys. Rev. Lett.* **110**, 095502 (2013).
- <sup>27</sup>D. Schick, M. Herzog, H. Wen, P. Chen, C. Adamo, P. Gaal, D. G. Schlom, P. G. Evans, Y. Li, and M. Bargheer, "Localized electric charge carriers generate ultrafast inhomogeneous strain in the multiferroic  $\text{BiFeO}_3$ ," *Phys. Rev. Lett.* **112**, 097602 (2014).
- <sup>28</sup>X. Huang, J. Safraneck, J. Corbett, Y. Nosochkov, J. Sebek, and A. Terebilo, "Low alpha mode for spear3," in *Proc. PAC07* (2007), pp. 1308–1310.
- <sup>29</sup>M. Abo-Bakr, J. Feikes, K. Hollmack, P. Kuske, W. B. Peatman, U. Schade, G. Wüstefeld, and H.-W. Hübers, "Brilliant, coherent far-infrared (THz) synchrotron radiation," *Phys. Rev. Lett.* **90**, 094801 (2003).
- <sup>30</sup>P. Kraft, A. Bergamaschi, C. Broennimann, R. Dinapoli, E. F. Eikenberry, B. Henrich, I. Johnson, A. Mozzanica, C. M. Schlepütz, P. R. Willmott, and B. Schmitt, "Performance of single-photon-counting pilatus detector modules," *J. Synchrotron Radiat.* **16**, 368–375 (2009).
- <sup>31</sup>J. F. Ihlefeld, N. J. Podraza, Z. K. Liu, R. C. Rai, X. Xu, T. Heeg, Y. B. Chen, J. Li, R. W. Collins, J. L. Musfeldt, X. Q. Pan, J. Schubert, R. Ramesh, and D. G. Schlom, "Optical band gap of  $\text{BiFeO}_3$  grown by molecular beam epitaxy," *Appl. Phys. Lett.* **92**, 142908 (2008).
- <sup>32</sup>S. K. Pandey, A. R. James, R. Raman, S. N. Chatterjee, A. Goyal, C. Prakash, and T. C. Goel, "Structural, ferroelectric, and optical properties of pzt thin films," *Physica B* **369**, 135–142 (2005).
- <sup>33</sup>T. Ejdrup, H. T. Lemke, K. Haldrup, T. N. Nielsen, D. A. Arms, D. A. Walko, A. Miceli, E. C. Landahl, E. M. Dufresne, and M. M. Nielsen, "Picosecond time-resolved laser pump/x-ray probe experiments using a gated single-photon-counting area detector," *J. Synchrotron Radiat.* **16**, 387–390 (2009).
- <sup>34</sup>See supplementary material at <http://dx.doi.org/10.1063/1.4875347> for derivation of this result.
- <sup>35</sup>B. Krenzer, A. Janzen, P. Zhou, D. von der Linde, and M. H. von Hoegen, "Thermal boundary conductance in heterostructures studied by ultrafast electron diffraction," *New J. Phys.* **8**, 190 (2006).